Theoretical studies on the complexation of uranyl with typical carboxylate and amidoximate ligands

ARTICLE *in* SCIENCE CHINA-CHEMISTRY · NOVEMBER 2013

Impact Factor: 1.7 · DOI: 10.1007/s11426-013-4994-6

4 AUTHORS, INCLUDING:

Jing Su
Shanghai Institute of Applied Physics
32 PUBLICATIONS **240** CITATIONS
SEE PROFILE

Jun li
Harbin Institute of Technology
251 PUBLICATIONS **7,270** CITATIONS
SEE PROFILE

SCIENCE CHINA
Chemistry

• ARTICLES •

doi: 10.1007/s11426-013-4994-6

Theoretical studies on the complexation of uranyl with typical carboxylate and amidoximate ligands

XU ChaoFei[1], SU Jing[2,3*], XU Xiang[1,4] & LI Jun[1*]

[1]*Department of Chemistry & Key Laboratory of Organic Optoelectronics and Molecular Engineering of the Ministry of Education, Tsinghua University, Beijing 100084, China*

[2]*Division of Nuclear Materials Science and Engineering, Shanghai Institute of Applied Physics, Chinese Academy of Sciences, Shanghai 201800, China*

[3]*Key Laboratory of Nuclear Radiation and Nuclear Energy Technology, Chinese Academy of Sciences, Shanghai 201800, China*

[4]*College of Chemistry and Pharmaceutical Sciences, Qingdao Agricultural University, Qingdao 266109, China*

Received August 28, 2013; accepted September 8, 2013

Understanding of the bonding nature of uranyl and various ligands is the key for designing robust sequestering agents for uranium extraction from seawater. In this paper thermodynamic properties related to the complexation reaction of uranyl(VI) in aqueous solution (i.e. existing in the form of $UO_2(H_2O)_5^{2+}$) by several typical ligands (L) including acetate ($CH_3CO_2^-$), bicarbonate ($HOCO_2^-$), carbonate (CO_3^{2-}), $CH_3(NH_2)CNO^-$ (acetamidoximate, AO^-) and glutarimidedioximate (denoted as GDO^{2-}) have been investigated by using relativistic density functional theory (DFT). The geometries, vibrational frequencies, natural net charges, and bond orders of the formed uranyl-L complexes in aqueous solution are studied. Based on the DFT analysis we show that the binding interaction between uranyl and amidoximate ligand is the strongest among the selected complexes. The thermodynamics of the complexation reaction are examined, and the calculated results show that complexation of uranyl with amidoximate ligands is most preferred thermodynamically. Besides, reaction paths of the substitution complexation of solvated uranyl by acetate and AO^- have been studied, respectively. We have obtained two minima along the reaction path of solvated uranyl with acetate, the monodentate-acetate complex and the bidentate-acetate one, while only one minimum involving monodentate-AO complex has been located for AO^- ligand. Comparing the energy barriers of the two reaction paths, we find that complexation of uranyl with AO^- is more difficult in kinetics, though it is more preferable in thermodynamics. These results show that theoretical studies can help to select efficient ligands with fine-tuned thermodynamic and kinetic properties for binding uranyl in seawater.

uranyl, seawater, carboxylate, amidoximate, complexation, thermodynamics, density functional theory

1 Introduction

Uranium is a valuable non-renewable energy resource for electric power supply in nuclear power plant, due to its advantages of economy, low-carbon emission and high energy density. Given the anticipated exhaustion of terrestrial uranium in the near future and the extremely huge amount of uranium in seawater (4.5 billion tons), extraction of uranium from seawater is expected as a rich supply for long-term nuclear power production [1, 2]. However, practical extraction of uranium from seawater faces huge challenges, because uranium exists in the form of a highly stable carbonate complexes at an extremely low concentration (~3 ppb) in the presence of many other metal ions of overwhelmingly high concentrations (i.e. Na^+, Mg^{2+}, Ca^{2+}, K^+, etc.) [3]. Therefore, to successfully extract uranium from seawater, the extractant must be highly efficient, specifically selective and virtually insoluble at the seawater pH (~8.3)

*Corresponding authors (email: sujing@sinap.ac.cn; junli@tsinghua.edu.cn)

and ionic strength, as well as highly recyclable for economy consideration.

Uranium presents in dominant form of $UO_2(CO_3)_3^{4-}$ complex (ca. 85%) in seawater with also other minority forms of $UO_2(CO_3)_2^{2-}$, $UO_2(OH)^+$, $UO_2(OH)_2$, and $UO_2(OH)_3^-$, depending on the seawater condition [4]. Experimentally, amidoxime-based sorbents prepared by radiation grafting have been demonstrated to show the best absorption activity for $UO_2(CO_3)_3^{4-}$ among many techniques, e.g. inorganic sorbents, biomass collection, solvent extraction and ion exchange [1, 5–12]. Marine experiments showed that uranium extraction efficiency increases when seawater temperature increases. Besides, wave and tidal motions strengthening also improves the adsorption rate [5, 6]. The crystal structure data indicate that the open chain diamidoxime ligands coordinate to uranium in a η^2 binding mode with N–O bond and that the cyclic imide dioxime in a tridentate mode via the two oxime oxygen atoms and the imide nitrogen atom [13, 14]. Experimental thermodynamic analyses confirmed that the overall sequestration of U(VI) from seawater by glutarimidedioxime is endothermic and can be enhanced at higher temperature [14]. However, it remains unclear why amidoxime-based functional group exhibits a superior uranium sequestering ability. The related theoretical chemistry investigations are rare, in spite of a few reports on the computational modeling of the coordination structures of uranyl amidoxime complexes [13–15].

The purpose of this paper is to provide a fundamental understanding for extraction of uranium from seawater through theoretical investigations of thermodynamic properties of the complexation reaction of uranyl(VI) in aqueous solution with several typical coordinating ligands. Through quantum chemical calculations, we have determined the energetics and vibrational frequencies. Thermodynamic enthalpies, entropies and Gibbs free energies are derived via statistical mechanics analysis. The temperature effect on the thermodynamic energies is included. Besides, the reaction paths of the complexation of uranyl(VI) by acetate and acetamidoximate are studied. The theoretical results are analyzed and discussed to understand the sequestering ability of these typical ligands and the extraction kinetics. Quantum chemical bond-order analyses are carried out to explore the essence of the extraction abilities of different ligands towards uranyl(VI).

2 Computational methods

The theoretical calculations were carried out by using the density functional theory (DFT) method implemented in the Gaussian 09 program [16], and the hybrid exchange-correlation functional B3LYP [17, 18] was employed. The Stuttgart energy-consistent relativistic pseudo-potential ECP60MWB and the ECP60MWB-SEG valence basis sets was applied for U [19–21], and the cc-pVDZ all-electron basis set [22] were applied for H, C, N and O. To account for solvation effects, we used the polarizable continuum model COSMO approach [23, 24]. The geometrical structures of $UO_2(H_2O)_5^{2+}$ and all the uranyl-L complexes mentioned above were fully optimized, and vibrational frequency analyses were calculated to confirm that they are stable minima on the potential energy surface. Natural population analyses (NPA) were carried out using the natural bond orbital (NBO) method [25] implemented in NBO 5.G program [26]. We also did single-point DFT/PBE [27] calculations to perform bond-order analyses using the Amsterdam density functional (ADF 2010.02) program [28–30]. In these calculations the Slater basis sets with the quality of triple-ζ plus two polarization functions (TZ2P) [31] were used, with the frozen core approximation applied to the inner shells [$1s^2$-$5d^{10}$] for U, and [$1s^2$] for C, O and N. The scalar relativistic (SR) effects were taken into account by the zero-order regular approximation (ZORA) [32]. Relativistic spin-orbit coupling effects were not considered due to the closed-shell nature of uranyl complexes.

3 Results and discussion

3.1 Geometry

The monovalent and divalent ligands we studied are shown in Figure 1, and the optimized structures of corresponding complexes are shown in Figure 2. The optimized geometries and vibrational frequencies are listed in Table 1. Here only five-coordination structures in the equatorial plane of uranyl, which have been confirmed to be most stable by experimental and theoretical studies [33–37], are considered. It is known that the axial and equatorial ligands compete the 5f/6d orbitals of uranium; the donation of electron to the U(VI) center by an equatorial ligand tends to enhance the uranyl-ligand binding and weakens the uranyl $U{\equiv}O_{ax}$ bonds [38–41]. In order to avoid the effect of the electrostatic attraction due to ligand carrying different charges, we selected the ligands with charges of –1 and –2, respectively.

In Table 1, the distances between uranium and the axial oxygen ($U–O_{ax}$) in $[UO_2(H_2O)_3(AO)]^+$ are longer than those in $[UO_2(H_2O)_n(CH_3CO_2)]^+$ and $[UO_2(H_2O)_n(HOCO_2)]^+$ (n = 3, 4) by 0.01–0.02 Å, indicating that the $U{\equiv}O_{ax}$ bonds are weakened more by AO^- coordination than by acetate and bicarbonate. Similarly, $U–O_{ax}$ distance is longer by 0.02 Å in $[UO_2(H_2O)_3(GDO)]$ than in $[UO_2(H_2O)_3(CO_3)]$, showing that GDO^{2-} coordination weakens $U{\equiv}O_{ax}$ bonds more than carbonate coordination. Therefore, for both the monovalent and divalent ligands, coordination of amidoximate-based ligands to uranyl donates more electron density to U than non-amidoximate-based ligands. Besides, there is an inverse correlation between bond lengths and symmetrical stretching frequencies of $U–O_{ax}$ (υ_s). Therefore, $\upsilon_s(U\text{-}O_{ax})$ also

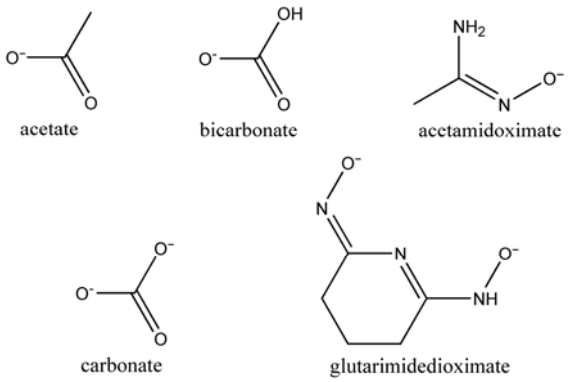

Figure 1 Monovalent ligands (acetate, bicarbonate, acetamidoximate) and divalent ligands (carbonate, glutarimidedioximate).

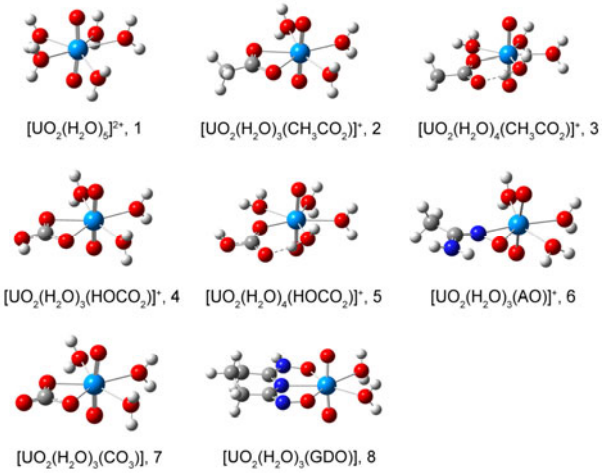

Figure 2 Optimized structures of complexes **1**–**8**.

reflects the superior binding strength of amidoximate-based ligands. The U–O_{ax} antisymmetrical frequencies (υ_s), also presented in Table 1, show the same trend as υ_s, which has been observed in other actinyl complexes as well [42, 43].

For the uranyl complexes listed in Table 1, the uranyl-oxygen (water) bond lengths (U–O_w) are in the range of 2.43–2.56 Å, which generally increase as U–O_w bond strength decreases and accordingly U–O_{ax} bond length increases. Two coordination modes, i.e. monodentate and bidentate, are found for $CH_3CO_2^-$ and $HOCO_2^-$ ligands. The formed complexes are distinctive in uranium-carbon (U–C) distances, 3.38 Å and 2.78 Å for the monodentate and bidentate complexes, respectively, which are consistent with the average results (at 3.5 and 2.87 Å) of experimental crystal/EXAFS data [44–49]. Additionally, the uranium-oxygen (ligand) bond length (U–O_L) is smaller for monodentate than for bidentate by 0.1 Å. For amidoximate-based ligands, the average U–O_L distance in the coordination complexes is around 2.26 Å, and a similar distance (2.29 Å) is obtained for CO_3^{2-} coordination. The uranium-nitrogen bond length (U–N) is 2.35 Å for bidentate ligand AO^-, while it is 2.47 Å for tridentate GDO^{2-}, in good agreement with the trend observed in related crystal structures [11,12] (around 2.37 and 2.56 Å, respectively). The average U–O distances in the equatorial plane for all the uranyl complexes in Table 1 are in the range of 2.46 to 2.42 Å, which become slightly shorter when anionic ligands replace neutral water for uranyl coordination.

3.2 Natural charge analyses and bond orders

The results of natural charge analyses for all the uranyl-L complexes are listed in Table 2. Clearly, U atom carries a large positive charge, which is influenced by the coordinating ligands, as found in uranium halide complexes [50, 51]. From Table 2, U atom in $[UO_2(H_2O)_3(AO)]^+$ complex carries less positive charges than those in $[UO_2(H_2O)_n(CH_3CO_2)]^+$ and $[UO_2(H_2O)_n(HOCO_2)]^+$ (n = 3, 4), revealing that more electron density donation from AO^- than from $CH_3CO_2^-$ and $HOCO_2^-$ to the U center. Similarly, for the complexes with doubly negatively charged ligands, U atom in $[UO_2(H_2O)_3(GDO)]$ complex carries less positive charges than that in $[UO_2(H_2O)_3(CO_3)]$ complex. The average negative charge on the coordinated ligand oxygen (O_L) atom is around –0.71 for carboxylate-based ligands and –0.55 for amidoximate-based ligands. The negative charge on the

Table 1 Optimized distances (in Å) between uranium and coordinated atom, U–O_{ax} (axial oxygen), U–O_w (water), U–O_L (ligand), U–O_{eq}, and U–N, and distances between uranium and carbon in carboxylate ligands U–C_L, O_{ax}–U–O_{ax} symmetrical and antisymmetrical stretching frequency (υ_s and υ_{as}) from COSMO DFT/B3LYP calculations of uranyl complexes

No.[a)]	L	Mode	U–O_t	U–O_w	U–O_L	U–N	U–C	U–O_{eq}[b)]	υ_s	υ_{as}
1	H_2O	–	1.75	2.43–2.51	–	–	–	2.46	912	972
2	$CH_3CO_2^-$	bi	1.76	2.46–2.47	2.40×2	–	2.79	2.44	888	948
3	$CH_3CO_2^-$	mono	1.77	2.44–2.52	2.27	–	3.39	2.44	882	944
4	$HOCO_2^-$	bi	1.76	2.45–2.46	2.41×2	–	2.78	2.44	892	951
5	$HOCO_2^-$	mono	1.76	2.43–2.51	2.30	–	3.37	2.44	888	949
6	AO^-	bi	1.78	2.50–2.52	2.24	2.35	–	2.44	854	914
7	CO_3^{2-}	bi	1.78	2.52	2.29×2	–	2.77	2.43	853	905
8	GDO^{2-}	tri	1.80	2.54–2.56	2.21, 2.36	2.47	–	2.42	824	874

a) See Figure 2 for the structure of complex **1**–**8**. b) Average of various U–O bond lengths in the equatorial plane.

Table 2 Natural net charges of uranium, ligand oxygen and ligand nitrogen

L	Mode	U	O_L	N_L
$CH_3CO_2^-$	bi	1.932	–0.664×2	–
	mono	1.931	–0.736	–
$HOCO_2^-$	bi	1.931	–0.701, –0.670	–
	mono	1.944	–0.768	–
AO^-	bi	1.821	–0.520	–0.294
CO_3^{2-}	bi	1.810	–0.736×2	–
GDO^{2-}	tri	1.775	–0.592, –0.529	–0.689

coordinated N atoms (N_L) of amidoximate-based ligands increases from –0.29 for bidentate AO^- to –0.69 for tridentate GDO^{2-}. These charge distribution results agree well with the donating ability of the ligands to uranyl.

Quantum chemical bond order is a measurement of the multiplicities of bonds, and is related to bond strength and relative stability when comparing similar bonding situation. The Nalewajski–Mrozek (N–M) bond orders [52] calculated for the complexes studied are listed in Table 3. Comparing the complexes with the same monovalent ligands, it is found that the average U–O_L bond orders of the complexes with the amidoximate-based ligand (1.40) are larger than those with carboxylate-based ligands (1.08 for bidentate and 1.30 for monodentate complexes). The same trend is observed for the summation of the U–L bond orders without inclusion of the contribution of the U–O_{ax} bond. A similar observation is found in the case of doubly negatively charged ligands. These results clearly show that the overall binding strength of equatorial ligands is much stronger in amidoximate-based complexes than in carboxylate-based complexes. That is, the amidoximate-based complexes are more stable than the carboxylate-based complexes listed in Table 3. Besides, in the amidoximate-based complexes, bond orders of U–O_L are larger than 1.0, while those of U–N_L are about 0.8, which corroborates that the U–O_L bond is stronger than the U–N_L bond. The Mayer bond order [53] and the Gophinatan- Jug (G-J) bond order [54] are also calculated and are not listed because they give the similar conclusion.

3.3 Thermodynamics

To examine the binding ability of various ligands towards uranyl in terms of thermodynamics , the complexation reaction Eq. (1) is introduced.

$$[UO_2(H_2O)_5]^{2+} + L^{2-/-} \leftrightarrow [UO_2(L)(H_2O)_n]^{0/+} + (5-n)\ H_2O \quad (1)$$

Through statistical mechanics analysis the thermodynamic data for these processes were calculated at 1 atm and 300 K using DFT/B3LYP functional and COSMO solvation model. The corresponding reaction energy ΔE, reaction enthalpy ΔH, Gibbs free energy ΔG and reaction entropy ΔS for the six uranyl complexation processes are given in Table 4. Here following thermodynamic convention, the negative ΔH and ΔG values show that the complexation reactions of uranyl by a ligand are exothermic and favorable in thermodynamics. For $CH_3CO_2^-$ and $HOCO_2^-$ ligands, the entropy values ΔS are negative for forming monodentate uranyl complexes, but positive for forming bidentate complexes. However, the more negative ΔG values for the former show that monodentate coordination is preferred by a enthalpy driven mechanism and the bidentate coordination is favorable in entropy. Comparing the ΔG values of the three complexes with the monovalent ligands, the complex with AO^- ligand gives the most negative value (–236.1 kJ/mol), indicating that it is most exothermic in thermodynamics. Similarly, comparing the three complexes with divalent ligands, the ΔG value of the complex with GDO^{2-} is more negative than CO_3^{2-} by a difference of 80 kJ/mol, indicating GDO^{2-} is more preferable in thermodynamics. Note that formation of the GDO^{2-} complex gives much smaller positive ΔS than the CO_3^{2-} complex, and therefore, the preference for the former is driven by enthalpy, similar as in the case of

Table 3 Nalewajski–Mrozek bond orders of uranyl complexes with various ligands

L	Mode	U–O_L(1)	U–O_L(2)	U–N_L	U_{sum} [a)]
$CH_3CO_2^-$	bi	1.078	1.078	–	2.547
	mono	1.321	–	–	2.581
$HOCO_2^-$	bi	1.074	1.074	–	2.533
	mono	1.288	–	–	2.551
AO^-	bi	1.396	–	0.773	2.768
CO_3^{2-}	bi	1.346	1.350	–	3.565
GDO^{2-}	tri	1.123	1.459	0.776	3.703

a) Summation of the bond orders without inclusion of the U–O_{ax} contribution.

Table 4 Thermodynamic data of complexation reaction (Eq. (1)) with different ligands: electronic reaction energy ΔE, reaction enthalpy H, Gibbs free energy G (including standard state correction [55]) and reaction entropy S from COSMO DFT/B3LYP calculations

L	Mode	ΔE (kJ/mol)	ΔH (kJ/mol)	ΔG (kJ/mol)	ΔS (J/K·mol)
$CH_3CO_2^-$	bi	–137.8	–130.3	–142.5	41.0
	mono	–186.8	–186.2	–162.5	–79.5
$HOCO_2^-$	bi	–114.4	–107.1	–117.9	36.5
	mono	–161.4	–160.9	–137.9	–77.2
AO^-	bi	–235.1	–228.1	–236.1	26.9
CO_3^{2-}	bi	–377.3	–372.3	–379.1	358.1
GDO^{2-}	tri	–442.1	–435.6	–459.8	81.2

monodentate coordination of $CH_3CO_2^-$ and $HOCO_2^-$ ligands.

Based on the calculated data, the temperature effects on the thermodynamics of complexation with AO^- and GDO^{2-} ligands are studied and shown in Figures 3 and 4, respectively. Interestingly, the calculated ΔG values of the two complexation reactions become more negative with the increase of the temperature, indicating that the complexation reactions are more favorable at higher temperature, consistent with experimental observation of uranium extraction from seawater [5, 6]. Comparing the these two plots, the ΔG value of the complex with GDO^{2-} ligand changes faster, indicating that the complexation reaction of $UO_2(H_2O)_5^{2+}$ by GDO^{2-} is affected more strongly by temperature change. One can therefore design ligands with larger entropy effect to influence the complexation processes via the favorable temperature effect. It is worth mentioning that the temperature effects on the thermodynamics of complexation with other ligands, which are not shown, give the similar conclusion.

3.4 Reaction paths of the complexation of solvated uranyl by CH_3COO^- and AO^-

In addition to the thermodynamics, one key factor that concerns the efficiency of uranium extraction from seawater is the kinetics of the extraction process. To study the reaction kinetics of the uranyl aqueous complex with various ligands, we performed a series of constrained optimizations via a linear transit scheme without any symmetry restrictions for a set of fixed distances between U and a selected atom of the ligand to plot the reaction path. The reaction path for the complexation of solvated uranyl $[UO_2(H_2O)_5]^{2+}$ by acetate is investigated by following the U–C distance over the range from 4.6 to 2.6 Å, and the results are shown in Figure 5. The reaction energy is determined based on the model reaction Eq. (1). All the structures involved in the reaction path are depicted in Figure 6. Our calculation results show that the complexation process starts from the outer-sphere uranyl-acetate complex, and successively forms the monodentate and bidentate complexes. According to Figure 5 the barrier from the out-sphere complex to the monodentate-acetate complex is estimated to be around 15 kJ/mol, and the barrier from the monodentate-acetate complex to the bidentate-acetate one is about 9 kJ/mol.

The reaction path of the complexation of solvated uranyl by AO^- is also investigated along the U–O_L distance decreasing from 3.9 to 2.2 Å, as is shown in Figure 7. Starting from the outer-sphere uranyl-AO complex, we only obtained one minimum in the energy surface, corresponding to the monodentate-AO complex shown in Figure 8. The fact that a bidentate-AO minimum is not located implies that

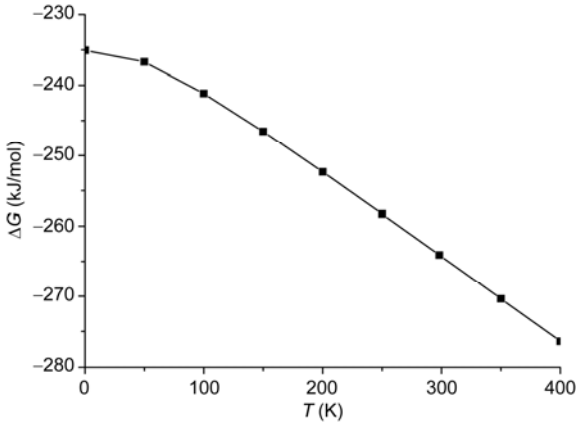

Figure 3 Plot of ΔG of the AO^- complexation reaction with the temperature change.

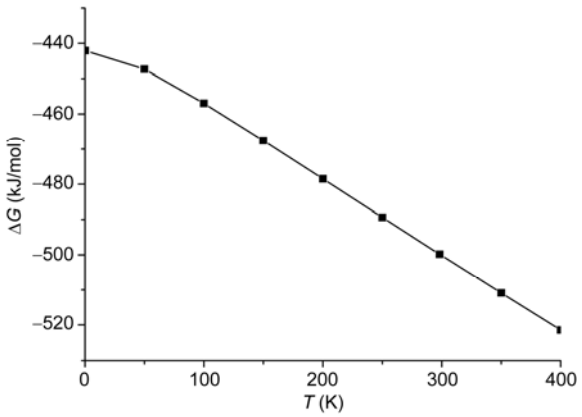

Figure 4 Plot of ΔG of the GDO^{2-} complexation reaction with the temperature change.

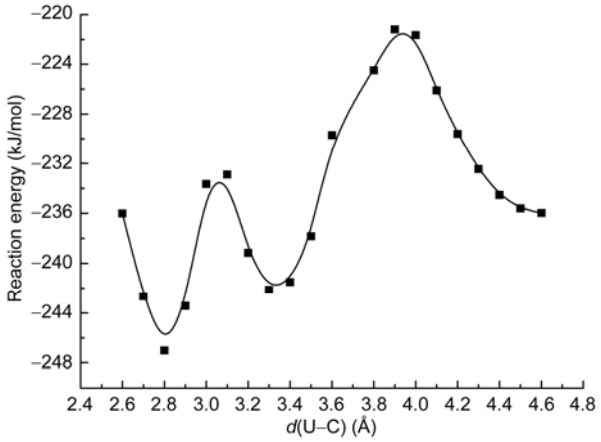

Figure 5 Reaction path of the complexation of aqueous solvated uranyl by acetate.

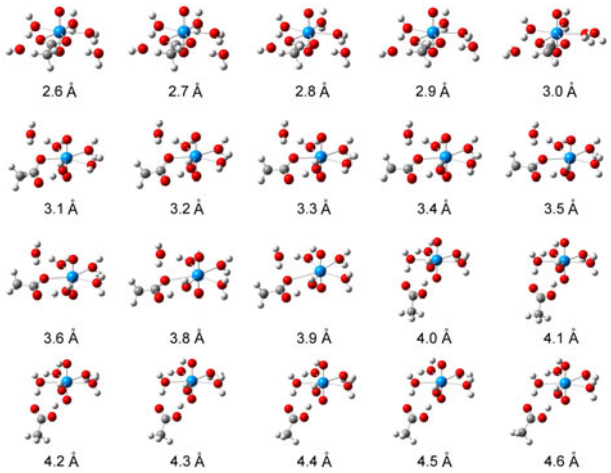

Figure 6 Restrictively optimized structures on the reaction path of the complexation of aqueous solvated uranyl by acetate.

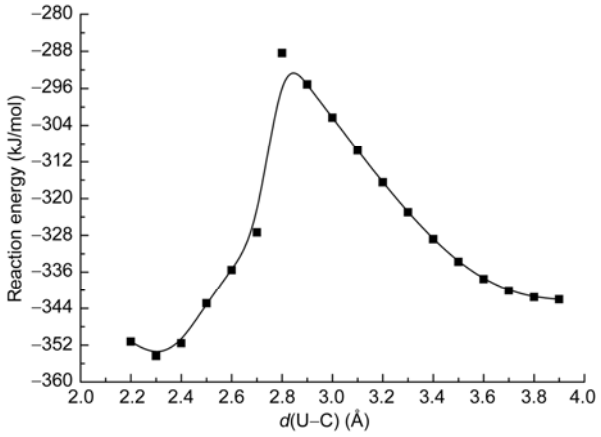

Figure 7 Reaction path of the complexation of solvated uranyl by acetamidoximate (AO^-).

such coordination mode is likely not favored due to significant difference in the binding ability of the N- and O-atom of AO^- ligand. The barrier of forming monodentate AO

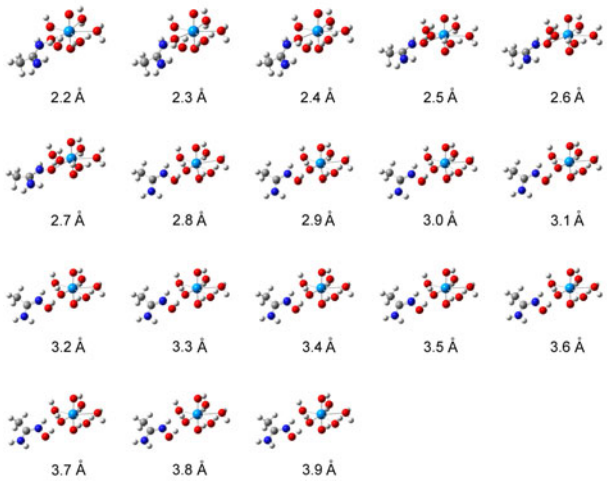

Figure 8 Restrictively optimized structures on the reaction path of the complexation of solvated uranyl by acetamidoximate (AO^-).

complex is about 54 kJ/mol, which is much higher than that for forming uranyl monodentate acetate complex. This result demonstrates that it is difficult and kinetically slow to sequester uranium by AO^-, though it is much more favorable thermodynamically than the carboxylate-based ligands. This is also consistent with the experimental observations of uranium extraction from seawater [5, 6, 14]. These results show that there is considerable space for improving the kinetics of uranium extraction from seawater via amidoxime-based ligands. Further theoretical study is ongoing to provide guidance for experimental design of robust ligands for uranium extraction from seawater.

4 Conclusions

In this paper, using relativistic DFT methods we have studied the coordination structures and thermodynamic properties of uranyl complexes with several typical ligands, including acetate ($CH_3CO_2^-$), bicarbonate ($HOCO_2^-$), carbonate (CO_3^{2-}), $CH_3(NH_2)CNO^-$ (acetamidoximate, AO^-), and glutarimidedioximate (GDO^{2-}). The geometrical structures and theormodynamic data are compared within the ligands of the same negative charges to avoid the effect of electrostatic attraction due to carrying different charges. Among monovalent complexes with the ligands of −1 charge, the axial uranium-oxygen ($U–O_{ax}$) bond length of complex with AO^- is longer than those of complexes with acetate and bicarbonate, and correspondingly the symmetric stretching vibrational frequencies $\nu_s(U–O_{ax})$ and the antisymmetric stretching vibrational frequencies $\upsilon_{as}(U–O_{ax})$ are lower, revealing the stronger binding ability of acetamidoximate towards uranyl. Investigations based on the natural charge analysis and bond order analysis reveal that U in $[UO_2(H_2O)_3(AO)]^+$ carries more positive charge, and this complex has a larger total bond order of $U–O_L$. All the

above-mentioned results corroborate that AO^- donates more electron density to U and forms a stronger interaction with U than bicarbonate and acetate. A similar conclusion is obtained among comparison of carbonate and GDO^{2-} ligands, that is, the GDO^{2-} ligand has stronger interaction with uranyl than carbonate.

The calculated results of complexation of $[UO_2(H_2O)_5]^{2+}$ with a variety of selected ligands show that the complexation with AO^- gives more negative *E*, *H* and *G* values than those with acetate and bicarbonate. Therefore the uranyl-AO complexation is more preferred thermodynamically. Similarly, the uranyl-GDO complexation is more preferred than the uranyl-carbonate one.

The linear transit calculations of the reaction paths of the $[UO_2(H_2O)_5]^{2+}$ complexation by acetate reveals that monodentate and bidentate acetate coordination complexes are successively formed with energy barrier about 15 and 9 kJ/mol, respectively. The reaction path of AO^- complexation shows only a monodentate coordination complex with an energy barrier about 54 kJ/mol, which is much higher than those of the reaction path of the acetate complexation. These studies indicate that it is less efficient to form a complex with AO^- in terms of kinetics, though it is preferable in thermodynamics.

Our results show that by determining the uranyl-ligand bond lengths, bond orders, charge distribution, vibrational frequencies as well as the thermodynamic and kinetic data, computational chemistry modeling can provide insights in designing robust ligands with improved binding strengths and better kinetic efficiency. The currently used amidoxime-based functional group possess good thermodynamic feature for binding uranyl. Improving the kinetics of the amidoxime-based functional group and finding new ligands with better thermodynamics and kinetics thus become the frontier in rational design of high-performance ligands for uranium extraction from seawater.

We acknowledge the financial support by the National Natural Science Foundation of China (NSFC) (20933003 and 91026003) to JL and the Strategic Priority Research Program of the Chinese Academy of Sciences (XDA02040104), NSFC (21201106) and the China Postdoctoral Science Foundation (2012M520297) to JS. The calculations were performed at the Supercomputer Center of the Computer Network Information Center, Chinese Academy of Sciences, the Shanghai Supercomputing Center, and the Tsinghua National Laboratory for Information Science.

1 Davies RV, Kennedy J, McIlroy RW, Spence R , Hill KM. Extraction of uranium from sea water. *Nature*, 1964, 203: 1110–1115

2 OECD. *Uranium 2009: Resources, Production and Demand*. OECD NEA Publication 6891. 2010, 456

3 Sodaye H, Nisan S, Poletiko C, Prabhakar S, Tewari PK. Extraction of uranium from the concentrated brine rejected by integrated. *Desalination,* 2009, (235): 9–32

4 Kim J, Tsouris C, Mayes RT, Oyola Y, Saito T, Janke CJ, Dai S, Schneider E, Sachde D. Recovery of uranium from seawater: A review of current status and future research needs. *Separ Sci Technol*, 2013, 48: 367–387

5 Shimizu T, Tamada M. Practical scale system for uranium recovery from seawater using braid type adsorbent. *Proceed Civil Engin Ocean*, 2004, 20: 617–622

6 Tamada M, Seko N, Kasai N, Shimizu T. Cost estimation of uranium recovery from seawater with system of braid type adsorbent. *Transact Atomic Energy Soc Japan*, 2006, 5: 358–363

7 Wazne M, Meng X, Korfiatis GP, Christodoulatos C. Carbonate effects on hexavalent uranium removal from water by nanocrystalline titanium dioxide. *J Hazar Mater,* 2006, 136: 47–52

8 Muzzarelli RAA. Potential of chitin/chitosan-bearing materials for uranium recovery: An interdisciplinary review. *Carbohyd Polym,* 2011, 84: 54–63

9 Manos MJ, Kanatzidis MG. Layered metal sulfides capture uranium from seawater. *J Am Chem Soc,* 2012, 134: 16441–16446

10 Acharya C, Chandwadkar P, Joseph D, Apte SK. Uranium (VI) recovery from saline environment by a marine unicellular cyanobacterium, *Synechococcus elongates*. *Radioanal Nucl Chem,* 2013, 295: 845–850

11 Das S, Pandey AK, Athawale AA, Subramanian M, Seshagiri TK, Khanna PK, Manchanda VK. Silver nanoparticles embedded polymer sorbent for preconcentration of uraniumfrom bio-aggressive aqueous media. *J Hazard Mater* 2011, 186: 2051–2059

12 Cao Q, Huang F, Zhuang Z, Lin Z. A study of the potential application of nano-$Mg(OH)_2$ in adsorbing lowconcentrations of uranyltricarbonate from water. *Nanoscale*, 2012, 4: 2423–2430

13 Vukovic S, Watson L A, Kang SO, Custelcean R, Hay BP. How amidoximate binds the uranyl cation. *Inorg Chem,* 2012, 51: 3855–3859

14 Tian G, Teat SJ, Zhang Z, Rao L. Sequestering uranium from seawater: Binding strength and modes of uranyl complexes with glutarimidedioxime. *Dalton Trans,* 2012, 41: 11579–11586

15 Chi FT, Li P, Xiong J, Hu S, Gao T, Xia XL, Wang XL. Density functional study of uranyl(VI) amidoxime complexes. *Chin Phys B,* 2012, 21: 093102

16 Frisch MJ, Trucks GW, Schlegel HB, Scuseria GE, Robb MA, Cheeseman JR, Scalmani G, Barone V, Mennucci B, Petersson GA, Nakatsuji H, Caricato M, Li X, Hratchian HP, Izmaylov AF, Bloino J, Zheng G, Sonnenberg JL, Hada M, Ehara M, Toyota K, Fukuda R, Hasegawa J, Ishida M, Nakajima T, Honda Y, Kitao O, Nakai H, Vreven T, Montgomery JrJA, Peralta JE, Ogliaro F, Bearpark M, Heyd JJ, Brothers E, Kudin KN, Staroverov VN, Kobayashi R, Normand J, Raghavachari K, Rendell A, Burant JC, Iyengar SS, Tomasi J, Cossi M, Rega N, Millam JM, Klene M, Knox JE, Cross JB, Bakken V, Adamo C, Jaramillo J, Gomperts R, Stratmann RE, Yazyev O, Austin AJ, Cammi R, Pomelli C, Ochterski JW, Martin RL, Morokuma K, Zakrzewski VG, Voth GA, Salvador P, Dannenberg JJ, Dapprich S, Daniels AD, Farkas Ö, Foresman JB, Ortiz JV, Cioslowski J, Fox DJ. Gaussian 09, Revision B.01. Gaussian, Inc., Wallingford CT, 2010

17 Becke AD. Density-functional exchange-energy approximation with correct asymptotic behavior. *Phys Rev A,* 1988, 38: 3098–3100

18 Lee C, Yang W, Parr RG. Development of the Colle-Salvetti correlation-energy formula into a functional of the electron density. *Phys Rev B*, 1988, 37: 785–789

19 Dolg M. *Energy-consistent Pseudopotentials of the Stuttgart/Cologne Group*. http://www.tc.uni-koeln.de/PP/clickpse.en.html. 2013-05-01

20 Cao X, Dolg M, Stoll H. Valence basis sets for relativistic energy-consistent small-core actinide pseudopotentials. *J Chem Phys,* 2003, 118: 487–496

21 Cao X, Dolg M. Segmented contraction scheme for small-core actinide pseudopotential basis sets. *J Molec Struct (THEOCHEM)*, 2004, 673: 203–209

22 Dunning TH. Gaussian basis sets for use in correlated molecular calculations. I. The atoms boron through neon and hydrogen. *J Chem Phys*, 1989, 90: 1007–1023

23 Klamt A, Schüürmann G. COSMO: A new approach to dielectric screening in solvents with explicit expressions for the screening energy and its gradient. *J Chem Soc, Perkin Trans*, 1993, 2: 799–805

24 Pye CC, Ziegler T. An implementation of the conductorlike screening model (COSMO) of solvation within the Amsterdam density functional (ADF) package. *Theor Chem Acc*, 1999, 101: 396–408

25 Weinhold F, Landis CR. Valency and Bonding. *A Natural Bond Orbital Donor-Acceptor Perspective*. Cambridge University Press, 2005

26 Glendening ED, Badenhoop JK, Reed AE, Carpenter JE, Bohmann JA, Morales CM, Weinhold F. NBO 5.G. Theoretical Chemistry Institute, University of Wisconsin, Madison, WI, 2004; http://www.chem.wisc.edu/nbo5. 2013-05-01

27 Perdew JP, Burke K, Ernzerhof M. Generalized gradient approximation made simple. *Phys Rev Lett,* 1996, 77: 3865–3868

28 See http://www.scm.com for ADF 2010.02, SCM, Theoretical Chemistry, Vrije Universiteit, Amsterdam, The Netherlands

29 Guerra CF, Snijders JG, te Velde G, Baerends EJ. Towards an order-N DFT method. *Theor Chem Acc,* 1998, 99: 391–403

30 Velde GT, Bickelhaupt FM, Baerends EJ, Guerra CF, van Gisbergen SJA, Snijders JG, Ziegler T. Chemistry with ADF. *J Comput Chem,* 2001, 22: 931–967

31 van Lenthe E, Baerends EJ. Optimized Slater-type basis sets for the elements 1–118. *J Comput Chem,* 2003, 24: 1142–1156

32 van lenthe E, Baerends EJ, Snijders JG. Relativistic regular two-component Hamiltonians. *J Chem Phys*, 1993, 99: 4597–4610

33 Neuefeind J, Soderholm L, Skanthakumar S. Experimental electron densities of aqueous uranyl(VI) solutions. *J Phys Chem A*, 2004, 108, 2733s

34 Ikeda-Ohno A, Hennig C, Tsushima S, Scheinost A C, Bernhard G, Yaita T. Speciation and structural study of U(IV) and -(VI) in perchloric and nitric acid solutions. *Inorg Chem,* 2009, 48: 7201–7210

35 Vallet V, Wahlgren U, Schimmelpfennig B, Moll H, Szabo Z, Grenthe I. Solvent effects on uranium (VI) fluoride and hydroxide complexes studied by EXAFS and quantum chemistry. *Inorg Chem,* 2001, 40: 3516–3525

36 Su J, Zhang K, Schwarz WHE, Li J. Uranyl-glycine-water complexes in solution: Comprehensive computational modeling of coordination geometries, stabilization energies, and luminescence properties. *Inorg Chem*, 2011, 50: 2082–2093

37 Ray RS, Krüger S, Rösch N. Uranyl monocarboxylates of aromatic acids: A density functional model study of uranyl-humate complexation. *Dalton Trans*, 2009: 3590–3589

38 Denning RG. Electronic structure and bonding in actinyl ions. *Struct. Bonding (Berlin),* 1992, 79: 215–276

39 Denning RG. Electronic structure and bonding in actinyl ions and their analogs. *J Phys Chem A,* 2007, 111: 4125–4143

40 Su J, Wang YL, Wei F, Schwarz WHE, Li J. Theoretical study of the luminescent states and electronic spectra of UO_2Cl_2 in an argon matrix. *J Chem Theory Comput,* 2011,7*:* 3293–3303

41 Schlosser F, Krüger S, Rösch N. A density functional study of uranyl monocarboxylates. *Inorg Chem,* 2006, 45: 1480–1490

42 Shamov GA, Schreckenbach G. Density functional studies of actinylaquo complexes studied using small-core effective core potentials and a scalar four-component relativistic method. *J Phys Chem A,* 2005, 109: 10961–10974

43 Sundararajan M, Sinha V, Bandyopadhyay T, Ghosh SK. Can functionalized cucurbituril bind actinylcations efficiently? A density functional theory based investigation. *J Phys Chem A*, 2012, 116: 4388–4395

44 Denecke MA, Reich T, Bubner M, Pompe S, Heise KH, Nitsche H, Allen PG, Bucher JJ, Edelstein NM, Shuh DK. Determination of structural parameters of uranyl ions complexed with organic acids using EXAFS. *J Alloys Compd,* 1998: 271-273: 123–127

45 Denecke MA, Pompe S, Reich T, Moll H, Bubner M, Heise KH, Nicolai R, Nitsche H. Measurements of the structural parameters for the interaction of uranium (VI) with natural and synthetic humic acids using EXAFS. *Radiochim Acta,* 1997, 79: 151–159

46 Denecke MA. Actinide speciation using X-ray absorption fine structure spectroscopy. *Coord Chem Rev*, 2006, 250: 730–754

47 Jiang J, Rao L, Di Bernardo P, Zanonato PL, Bismondo A. Complexation of uranium(VI) with acetate at variable temperatures. *J Chem Soc, Dalton Trans,* 2002, 8: 1832–1838

48 Moll H, Geipel G, Reich T, Bernhard G, Fanghänel T, Grenthe I. Uranyl(VI) complexes with alpha-substituted carboxylic acids in aqueous solution. *Radiochim Acta,* 2003, 91, 11–20

49 Allen PG, Bucher JJ, Shuh DK, Edelstein NM, Reich T. Investigation of aquo and chloro complexes of UO_2^{2+}, NpO_2^{+}, Np^{4+}, and Pu^{3+} by X-ray absorption fine structure spectroscopy. *Inorg Chem,* 1997, 36: 4676–4683

50 Su J, Dau P D, Qiu YH, Liu HT, Xu CF, Huang DL, Wang LS, Li J. Probing the electronic structure and chemical bonding in tricoordinate uranyl complexes $UO_2X_3^-$ (X = F, Cl, Br, I): competition between coulomb repulsion and U–X bonding. *Inorg Chem,* 2013, 52: 6617–6626

51 Su J, Dau PD, Xu CF, Huang DL, Liu HT, Wei F, Wang LS, Li J. A joint photoelectron spectroscopy and theoretical study on the electronic structure of UCl_5^- and UCl_5. *Chem Asian J,* 2013, 8: 2489–2496

52 Michalak A, DeKock RL, Ziegler T. Bond multiplicity in transition-metal complexes: applications of two-electron valence indices. *J Phys Chem A*, 2008, 112: 7256–7263

53 Mayer I. Charge, bond order and valence in the *ab initio* SCF theory. *Chem Phys Lett,* 1983, 97: 270–274

54 Gopinathan MS, Jug K. Valency. I. A quantum chemical definition and properties. *Theor Chim Acta,* 1983, 63: 497–509

55 Kremleva A, Krüger S, Rösch N. Role of aliphatic and phenolic hydroxyl groups in uranyl complexationby humic substances. *Inorg Chem Acta*, 2009, 362: 2542–2550